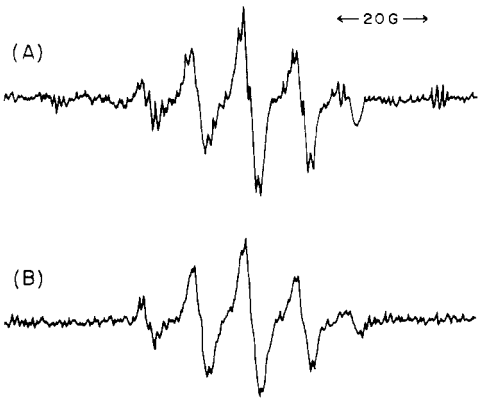

Figure 3. ESR spectra observed during pyrolysis at 94 °C (A) and photolysis at 25 °C (B) of MAIB in the presence of MMA in toluene. Reaction time: (A) 12 and min (B) 25; [MAIB] = 2 M, [MMA] = 4 M.

radical even after a long time, and absorptions corresponding to radical VIII were not detected. This is compatible with the low disproportionation/recombination ratio (≤ 0.11)[3] of the rates (k_d/k_c) of the primary radical-radical reaction for AIBN.

The quintet of quartets with high intensity is observed in the ESR spectra of the decompositions of MAIB in the presence of MMA as shown in Figure 3. Such acceleration was not observed in the ESR spectra when methyl acrylate and *p*-methoxystyrene were added to a MAIB solution as predicted from the reaction scheme. It is reasonable to consider that the persistent polymer radicals IX and X are also contained in these systems since the polymer was precipitated by pouring the reaction mixture into methanol, in contrast to the case in the absence of MMA, and k_d/k_c ratio of the termination in the polymerization of MMA is high, 1.9 at 25 °C[8] and 2.6 at 80 °C.[9] Polymerization of MMA by AIBN also gave a similar quintet of quartets in the ESR spectrum although its intensity was low.

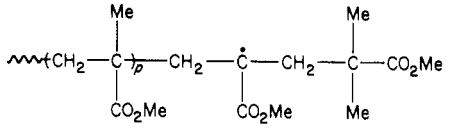

IX

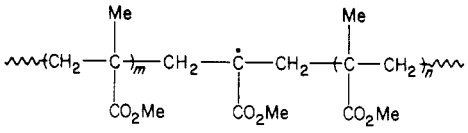

X

Although the present work was carried out under limiting conditions such as high concentration of initiator and low [monomer]/[initiator] ratio, the results obtained here will be helpful in understanding the elemental reactions of the polymerizations of methacrylates and their polymer structures as well as the decomposition mode of azo compounds, especially in high concentrations of initiator.

Registry No. MAIB, 2589-57-3; MMA, 80-62-6.

References and Notes

(1) Ranby, B.; Rabek, J. F. "ESR Spectroscopy in Polymer Research"; Springer-Verlag: New York, 1977. Tanaka, H.; Sato, T.; Otsu, T. *Makromol. Chem.* **1980**, *181*, 2421. Kamachi, M.; Kohno, M.; Liaw, D. J.; Katsuki, S. *Polym. J.* **1978**, *10*, 69.
(2) Tanaka, H.; Ota, T. *J. Polym. Sci., Polym. Lett. Ed.* **1985**, *23*, 93. Tanaka, H.; Sakai, I. Ota, T. *J. Am. Chem. Soc.*, accepted for publication.
(3) Tanaka, H.; Fukuoka, K.; Ota, T. *Makromol. Chem., Rapid Commun.* **1985**, *6*, 563.
(4) T. Sato and co-workers, unpublished data. This radical was generated from the radical polymerization of di-*n*-butyl itaconate in chlorobenzene at 127 °C, where the substituent R may be the Me_3CO group from the initiator (di-*tert*-butyl peroxide) since the reaction was carried out above the ceiling temperature of the monomer. Recently, Dr. M. Kamachi and his colleagues obtained similar ESR results in the polymerization of the same monomer at low temperature (−40 to +15 °c): Preprint of the 31st Kobunshi kenkyuhappyokai, Kobe, 1985, p 32.
(5) Schluter, K.; Berndt, A. *Tetrahedron Lett.* **1979**, 929.
(6) Pryor, W. A. "Free Radicals"; McGraw-Hill: New York, 1966.
(7) NMR spectra of this trimer (VI, colorless liquid) confirmed the assigned structure: ^{1}H NMR (400 MHz, $CDCl_3$) δ 1.01 (s, 3 H), 1.04 (s, 3 H), 1.16 (s, 3 H), 1.20 (s, 3 H), 1.25 (s, 3 H), 2.13 (d, J = 14 Hz, 1 H), 2.51 (d, J = 14 Hz, 1 H), 3.643 (s, 3 H), 3.645 (s, 3 H), 3.655 (s, 3 H); ^{13}C NMR (22.6 MHz, $CDCl_3$) δ 15.78 (q), 21.12 (q), 21.40 (q), 21.87 (q), 30.74 (q), 41.29 (s), 41.99 (t), 49.28 (s), 49.70 (s), 51.69 (q), 51.77 (q, 2 C), 175.84 (s), 175.89 (s), 178.95 (s).
(8) Bamford, C. H.; Dyson, R. W.; Eastmond, G. C. *Polymer* **1969**, *10*, 885.
(9) Schulz, G. V.; Henrici-Olive, G.; Olive, S. *Makromol. Chem.* **1959**, *31*, 88.

Hitoshi Tanaka,* Takashi Kagawa, Tsuneyuki Sato, and Tadatoshi Ota

Department of Applied Chemistry
Faculty of Engineering
Tokushima University, Tokushima 770, Japan

Received October 16, 1985

Adam-Gibbs Formulation of Nonlinearity in Glassy-State Relaxations

Relaxation in and below the glass transition temperature range is both nonexponential and nonlinear. The nonexponential character is conveniently and accurately described by the response function

$$\phi(t) = \exp[-(t/\tau_0)^\beta] \qquad 1 \geq \beta > 0 \qquad (1)$$

where τ_0 is a characteristic relaxation time and β is a measure of nonexponentiality. The nonlinear character is most conveniently treated by the method introduced by Tool[1] and generalized by Narayanaswamy,[2,3] in which τ_0, or some other characteristic time, is made a function of the departure from equilibrium. A commonly used functional form is the Narayanaswamy expression (N)

$$\tau_0 = A \exp\left[\frac{x\Delta h^*}{RT} + \frac{(1-x)\Delta h^*}{RT_f}\right] \qquad (2)$$

where A, x, and Δh^* are constants, R is the ideal gas constant, and T_f is the fictive temperature introduced by Tool.[4] Several investigators[5-12] have shown that Boltzmann superposition of eq 1 and 2 describes enthalpy relaxation during cooling, annealing, and heating with reasonable accuracy. However, eq 2 has several shortcomings:

(1) It predicts an Arrhenius temperature dependence for the equilibrium state, in conflict with the well-established WLF or Fulcher temperature dependences. Associated with this are unphysically large values of Δh^* (values as high as 450 kcal mol^{-1} have been reported).

(2) The nonlinearity parameter x has no clear physical interpretation.

(3) The physical significance (if any) of the strong inverse correlation between x and Δh^* [11] is unknown.

(4) The parameter x varies systematically with aging time and temperature.[13]

Recently, Scherer[14] has proposed the Adam-Gibbs equation[15] as a theoretical basis for treating nonlinearity.

0024-9297/86/2219-0936$01.50/0

In this Communication I develop this approach and demonstrate that it resolves many of the difficulties of eq 2.

The Adam–Gibbs expression for the relaxation time τ_0 is

$$\tau_0 = A' \exp\left[\frac{\Delta\mu s_c^*}{kTS_c}\right] \tag{3}$$

where $\Delta\mu$ is the free-energy barrier hindering rearrangement of a group of molecules, s_c^* is the configurational entropy of the smallest group capable of rearranging, and S_c is the macroscopic configurational entropy. Following Scherer,[14] we make S_c a function of fictive temperature:

$$S_c = \int_{T_2}^{T_f} \frac{C_{p,c}}{T}\, dT \tag{4}$$

where the lower integration limit T_2 is the configurational ground-state temperature and $C_{p,c}$ is the configurational contribution to the isobaric heat capacity. The appearance of T_f in eq 4 expresses the idea that the frozen-in residual entropy of a glass corresponds to the glassy value of T_f ($=T_f'$) and that it is the frozen-in entropy which determines the relaxation time in the glassy state. The value of $C_{p,c}$ is often equated to the change in heat capacity at T_g, ΔC_p, although Goldstein[16] has pointed out that vibrational degrees of freedom may contribute significantly to ΔC_p at T_g. We adopt a phenomenological approach and put $C_{p,c} = C/T$, whence

$$S_c = C\left[\frac{1}{T_2} - \frac{1}{T_f}\right] \tag{5}$$

Insertion of eq 5 into eq 3 and combining $\Delta\mu$, s_c^*, T_2, and C into one parameter $D = \Delta\mu s_c^* T_2/C$ gives

$$\tau_0 = A' \exp\left[\frac{D}{RT(1 - T_2/T_f)}\right] \tag{6}$$

In the equilibrium state ($T_f = T$) this assumes the form of the Fulcher equation

$$\tau_0 = A' \exp\left[\frac{D}{R(T - T_2)}\right] \tag{7}$$

As is well-known, eq 7 transforms to the WLF equation if T_2 is less than T_g by an amount C_2. We shall refer to eq 6 as the Adam–Gibbs–Fulcher (AGF) equation. Other functional forms for $\tau_0(T,T_f)$ can be obtained from different assumed temperature dependences of $C_{p,c}(T)$ but will not be considered here.

Approximate relationships between the AGF and N parameters can be derived by appropriate differentiation of eq 2 and 6. In the equilibrium state

$$\Delta h^* = R\frac{d \ln \tau_0}{d(1/T)} = D/(1 - T_2/T)^2 \tag{8}$$

In the glassy state ($T_f = T_f'$ = constant)

$$x\Delta h^* = R\frac{\partial \ln \tau_0}{\partial(1/T)}\bigg|_{T_f=T_f'} = D/(1 - T_2/T_f') \tag{9}$$

In the glass transition region $T \approx T_f' \approx T_g$, and elimination of Δh^* between eq 8 and 9 gives

$$x \approx 1 - T_2/T_g \tag{10}$$

Equations 8 and 10 give

$$\Delta h^* \approx D/x^2 \tag{11}$$

Equations 6–11 resolve many of the problems associated with the Narayanaswamy function. We have noted already the correct Fulcher/WLF form of eq 6 in the equilibrium state. In addition, eq 11 predicts that Δh^* at T_g should be larger for smaller values of x, if D is relatively constant. This is consistent with the observed inverse correlation between x and Δh^*[11] (see below for further discussion) and can account for the very large values of Δh^* associated with small values of x.[9,11]

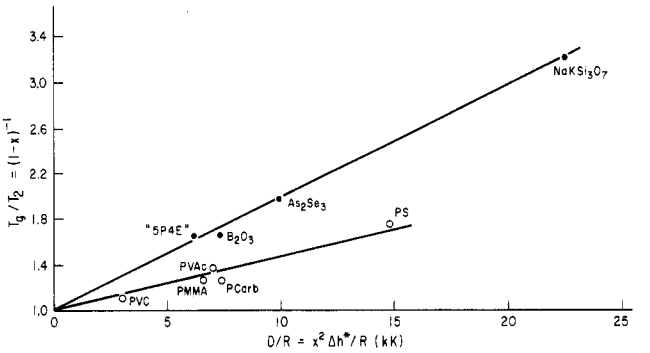

Figure 1. Variation of T_g/T_2 with D, calculated by using eq 10 and 11 and the Narayanaswamy parameters tabulated in ref 11. Abbreviations: "5P4E" = 5-phenyl-4-ether (see ref 6), PCarb = bisphenol A polycarbonate, PMMA = poly(methyl methacrylate), PS = polystyrene, PVAc = poly(vinyl acetate), and PVC = poly(vinyl chloride). See ref 11 for molecular weight and molecular weight distribution information. Narayanaswamy parameters for $NaKSi_3O_7$ taken from ref 6.

Equation 10 indicates that the N parameter x is a measure of how close T_g is to T_2. This suggests that as T_g approaches T_2 and the number of thermally accessible configurations is reduced, the relaxation time becomes increasingly dependent on structure and x decreases. Factors that may determine T_g/T_2 are discussed later. Equation 10 also accounts for systematic changes in x with aging time and temperature,[13] since as T_f relaxes during aging the ratio T_f/T_2 decreases and x becomes smaller.

Equations 8 and 10 allow D and T_g/T_2 to be estimated from published Narayanaswamy parameters. Figure 1 is a plot of T_g/T_2 vs. D calculated from data tabulated by Hodge.[11] Well-defined linear correlations are observed between D and T_g/T_2 for both polymeric and inorganic/monomeric glasses, but the two types of materials lie on distinctly different correlation lines. Extrapolations of both lines pass close to $T_g/T_2 = 1.0$ at $D = 0$, consistent with the expectation that T_g would approach T_2 as $\Delta\mu$ approached zero. Note that although D includes factors other than $\Delta\mu$, all these additional factors are finite and nonzero, so that $D \to 0$ corresponds unambiguously to $\Delta\mu \to 0$.

Comparison of the data tabulated in ref 11 and those in Figure 1 reveals that D and Δh^* are inversely related. Mathematically, this occurs because the product $x\Delta h^*$ is relatively constant[11] ($=K$, say) so that $D \approx x^2\Delta h^* \approx K^2/\Delta h^*$. Physically, it suggests that as $\Delta\mu$ decreases and T_g approaches T_2, the value of Δh^* is increased more by configurational constraints than it is decreased by its proportionality to $\Delta\mu$; i.e., relaxation becomes more cooperative as T_g approaches T_2. This can also account for the observed correlation between the nonexponentiality parameter β (eq 1), x, and Δh^*,[11] if it is assumed that lower values of β reflect higher degrees of cooperativity.

Finally, we note that the distinction between polymeric and inorganic/monomeric glasses seen in Figure 1 contrasts with the correlation between x and Δh^* observed earlier,[11] in which both types of material lay on the same correlation line. It is possible that D and T_g/T_2 reflect fundamental molecular differences between polymeric and inorganic/

monomeric glasses that Δh^* and x do not. The differences are such that comparable values of D correspond to larger values of T_g/T_2 for the inorganic/monomeric glasses. We speculate that, to the extent that D is a good measure of $\Delta\mu$, these differences may reflect three-dimensional configurational constraints for the inorganic/monomeric glasses that prevent them from approaching T_2 as closely as polymers, whose constraints are closer to being one-dimensional and may therefore be less restrictive.

Applications of eq 6 to experimental data, investigation of other functional forms generated from different assumed temperature dependences of $C_{p,c}$, and tests of eq 8–11 are in progress. The results of these studies, together with a more detailed consideration of the AGF formalism and its implications, will be reported elsewhere.[17]

Acknowledgment. I thank G. W. Scherer for stimulating discussions and preprints of ref 14.

References and Notes

(1) Tool, A. Q. *J. Am. Ceram. Soc.* **1946**, *29*, 240.
(2) Gardon, R.; Narayanaswamy, O. S. *J. Am. Ceram. Soc.* **1970**, *53*, 380.
(3) Narayanaswamy, O. S. *J. Am. Ceram. Soc.* **1971**, *54*, 491.
(4) Tool, A. Q.; Eichlin, C. G. *J. Am. Ceram. Soc.* **1931**, *14*, 276.
(5) DeBolt, M. A.; Easteal, A. J.; Macedo, P. B.; Moynihan, C. T. *J. Am. Ceram. Soc.* **1976**, *59*, 16.
(6) Moynihan, C. T.; Macedo, P. B.; Montrose, C.; Gupta, P. K.; DeBolt, M. A.; Dill, J. F.; Dom, B. E.; Drake, P. W.; Easteal, A. J.; Elterman, P. B.; Moeller, R. P.; Sasabe, H.; Wilder, J. A. *Ann. N.Y. Acad. Sci.* **1976**, *279*, 15.
(7) Sasabe, H.; Moynihan, C. T. *J. Polym. Sci.* **1978**, *16*, 1447.
(8) Moynihan, C. T.; Easteal, A. J.; Tran, D. C.; Wilder, J. A.; Donovan, E. P. *J. Am. Ceram. Soc.* **1976**, *59*, 137.
(9) Hodge, I. M.; Berens, A. R. *Macromolecules* **1982**, *15*, 762.
(10) Hodge, I. M.; Huvard, G. S. *Macromolecules* **1983**, *16*, 371.
(11) Hodge, I. M. *Macromolecules* **1983**, *16*, 898.
(12) Moynihan, C. T.; Bruce, A. J.; Gavin, D. L.; Loehr, S. R.; Opalka, S. M.; Drexhage, M. G. *Polym. Eng. Sci.* **1984**, *24*, 1117.
(13) Prest, W. M., Jr.; Roberts, F. J., Jr.; Hodge, I. M. "Proceedings of the Twelfth North American Thermal Analysis Society Conference", Williamsburg, VA, 1983, p 119.
(14) Scherer, G. W. *J. Am. Ceram. Soc.* **1984**, *67*, 504.
(15) Adam, G.; Gibbs, J. H. *J. Chem. Phys.* **1965**, *43*, 139.
(16) Goldstein, M. *J. Chem. Phys.* **1976**, *64*, 4767.
(17) Hodge, I. M., in preparation.
(18) This work was done while the author was at the BFGoodrich Research and Development Center, Brecksville, OH 44141.

I. M. Hodge[18]
Research Laboratories, Eastman Kodak Company
Rochester, New York 14650

Received October 2, 1985

Spherulites of Poly(L-histidine hydrochloride)

A histidine residue is an essentil constituent of the active site of several enzymes and plays a significant role in enzymic reaction, and it is also a ligand in some important metalloproteins.[1] Therefore the catalytic action of poly(L-histidine) (PLH) and its ligand characteristics have been the subject of intensive studies as a model for proteins with histidyl groups.[2] The interaction of PLH with DNA has also been examined.[3] Recently histidine-rich protein (HRP) has been found in the intraerythrocytic stages of development of the malaria parasite *Plasmodium lophurae* in ducks. Kilejian reported that HRP acts as an antigen and suggested the possibility of synthesizing malaria vaccine based on HRP,[4] though others have challenged this observation.[5] HRP comprises 73% histidine, and the histidine residues are incorporated almost exclusively as pentamers to nonamers in tandemly repeated units. The four major amino acid residues other than histidine (Ala, Glu, Pro, and Asp) link oligohistidines.[6] Thus PLH is regarded as a significant structural model of HRP as well.

Despite extensive investigations, no definite consensus seems to have been drawn as to the structure of PLH in aqueous alkaline solution,[7] while a recent Raman examination has led to the conclusion that PLH ($\bar{M}_w$ = 5000) assumes the β-form in aqueous gel at pH >6.5.[8] On the other hand, it is believed that PLH adopts a random conformation in acidic media.[7] From an infrared study, it was inferred that, in solid films, neutral PLH assumes the α-helical-form, and its hydrochloride presumably a random form.[9]

We have found that poly(L-histidine hydrochloride) crystallizes from aqueous solution in the form of negative spherulites large enough for an X-ray diffraction study. Here we propose that the left-handed 15/4 helix is a plausible structure of PLH hydrochloride based on its X-ray fiber photograph, its IR spectrum, and conformational energy calculation.

PLH[10] ($\bar{M}_n = 1.4 \times 10^4$, $\bar{M}_w/\bar{M}_n = 1.43$[11]) was dissolved in a slight excess of 1 N HCl, and the solution was lyophilized to yield white chips which contained 1 equiv of Cl^- and 1 mol of hydration water per residue as in the literature.[10] One milligram of the hydrochloride was placed on a glass slide (18 × 18 mm), 0.2 mL of distilled water was added to give a clear solution, and the mixture was spread over the slide. The solution was covered with a petri dish (2 × 10 cm) with a small vessel containing ca. 1 mL of water beside the slide and allowed to stand at room temperature (ca. 25 °C). After several days, the surface of the slide became opaque due to the growth of spherulites. For X-ray diffraction measurements, crystals developed on the glass slide were peeled off by the use of a sharp blade. A piece of the spherulite (10 × 500 μm) was attached at the tip of a steel needle and held in front of a collimeter (diameter, 100 μm). A micro flat-plate camera was used to take an X-ray diffraction photograph with an unfiltered microbeam of X-rays from Cu generated through a Rotaflex instrument (Rigaku Corp., Tokyo) at 45 kV and 200 mA.

In a photograph of the spherulite taken between crossed polaroids, a Maltese cross was observed (Figure 1). The spherulites showed negative birefringence, implying the molecular axis to lie in the tangential direction. The spherulites (KBr disk) showed an amide I IR band at 1653 cm^{-1} with a shoulder around 1680 cm^{-1} and an amide II band at 1527 cm^{-1}. This profile was same as that obtained from the film[9] and differed from those of either the α-helix or the β-form.[12] Further an amide I Raman line of spherulites appeared at 1686 cm^{-1},[13] which was also explicitly different from those of the α-helix, the β-form, and even the random coil.[14]

An X-ray fiber pattern was obtained by irradiating an X-ray beam normal to the surface at the circumference (Figure 2). The Bragg spacings of this diffraction pattern were indexed to a quasi-hexagonal lattice with $a = b =$ 14.95 Å, c = 45.0 Å, and γ = 116.5° (Table I) using Mitsui's graphical method.[15] The c axis lies tangential to the spherulite radius. The density was calculated to be 1.55 g cm^{-3} assuming that a unit cell contains three polymer chains, each residue of which is associated with 1 equiv of Cl^- and 1 mol of hydration water. This is not inconsistent with the observed density (1.44 g cm^{-3}).

The conformation of the polymer is a 15/4 helix with a monomer repeat of 3.00 Å. On the basis of standard values of bond lengths and bond angles of the main-chain

0024-9297/86/2219-0938$01.50/0